Laser and Particle Beams (2009), *27*, 103–108. Printed in the USA.

doi:10.1017/S0263034609000159

Surface morphology modifications of human teeth induced by a picosecond Nd:YAG laser operating at 532 nm

B.M. MIRDAN,[1] H.A. JAWAD,[1] D. BATANI,[2] V. CONTE,[3] T. DESAI,[2] AND R. JAFER[2]

[1]Institute of Laser for Postgraduate Studies, University of Baghdad, Baghdad, Iraq
[2]Dipartimento di Fisica "G.Occhialini," Università di Milano Bicocca, Milano, Italy
[3]Dipartimento di Morfologia Umana, Università di Milano, Milano, Italy

(RECEIVED 11 August 2008; ACCEPTED 26 November 2008)

Abstract

The interaction of an Nd:YAG laser, operating at 532 nm with 40 ps pulse duration, with human teeth was studied. The results show that teeth were significantly modified at an energy fluence of about 11 J/cm^2. Various surface morphologies of enamel and dentine were recorded. Features on enamel include crater (conical form) in the central part and cauliflower morphology at the periphery, whereas on dentine the crater looks like a stretched dome between sharp edges. The behavior of the enamel-dentine junction area showed different morphology with respect to both tooth enamel and dentine alone. Finally, the junction channel showed a removal of collagen fibers and the formation of a needle-like bottom structure. Generally, this investigation showed that the picosecond Nd:YAG laser can ablate a tooth surface practically instantaneously, implying that large tooth surfaces can be processed in short time.

Keywords: Biomaterials; Crater formation; Endodontics/human teeth; Laser treatment; Picosecond Nd:YAG laser

INTRODUCTION

Studies on surface modifications of various materials (including bio-materials) by different types of lasers are almost as old as the laser itself, and the field is constantly growing (Di Bernardo *et al.*, 2003; Bussoli *et al.*, 2007; Alti & Khare, 2006; Bashir *et al.*, 2007; Beilis, 2007; Batani *et al.*, 2003, 2007; Desai *et al.*, 2008, 2007, 2005; Fernandez *et al.*, 2005; Kasperczuk *et al.*, 2008; Schade *et al.*, 2006; Thareja & Sharma, 2006; Trusso *et al.*, 2005; Trtica *et al.*, 2006*a*, 2006*b*; Veiko *et al.*, 2006; Wieger *et al.*, 2006; Schreiber, 2005).

Various lasers and bio-materials have been used up to now for such studies. For fundamental and application interest, laser surface modification studies of bio-material including human teeth are very importance.

The tooth structure is known to be inhomogeneous and birefringent (Carlson & Krause, 1985; Zip & Bosch, 1993; Bhaskar, 1991), the coronal portion of the tooth can be regarded as a bio-mechanical complex of two major tissues: enamel and dentine. Enamel is the outermost layer restricted to the coronal portion of the tooth. It is composed of enamel rods, which are not in direct contact with each other, but are cemented together by inter-prismatic substance. Dentine is the supporting structure and consists of specialized cells and bulky intercellular substance. The latter consists of two components: (1) collagenous fibers and (2) cementing substance mainly composed of polysaccharides (Bhaskar, 1991; Takuma *et al.*, 1982).

The specialized cells are the odontoblasts. Each cell consists of two parts, the body of the cell that lies in the pulpal side of dentine and the odontoblastic process that extends through the full thickness of the dentine (the so-called, Tom's fiber) in the dentinal tubules. Each odontoblastic process in the dentine is found in thin walled tubes. The wall (the so-called Newman's sheath) is not formed by a different membrane, but originates from the differences in the nature of the matrix at the edge of the tubules, or from differences in the orientation of the fibers.

The interest in the studies of laser beam interaction with human teeth has risen, especially in the last two decades; Nd:YAG (Serafetinides *et al.*, 1999), Ti:Sapphire (Rode *et al.*, 2003), TEA CO_2 (Makropoulou *et al.*, 1996), and different excimer (Neev *et al.*, 1993; Frankline *et al.*, 2005) laser systems have so far been employed for these purposes.

Generally, during laser interaction with tooth surfaces, the laser energy is partially absorbed, and partially reflected. Due

Address correspondence and reprint requests to: B.M. Mirdan, Institute of Laser for Postgraduate Studies, University of Baghdad, Baghdad, Iraq. E-mail: balsammardan@gmail.com

to the high intensity laser interaction, the initially absorbed part induces multiphoton absorption (MPA) and multiphoton ionization (MPI). Free electrons generated by means of multiphoton absorption will absorb the energy from the laser light, initiating ionization avalanche, and producing an exponential growth of free electron. Consequently, laser absorption increases exponentially as well. Due to the high laser intensity and the key role of MPA, even transparent materials become strongly absorbent, independently of the linear absorption characteristics (Neev *et al.*, 1996).

Again, in general, interaction of a short duration laser pulse with the target minimizes thermal and hydrodynamic effects (melting, shock waves propagation, etc.). However, interaction of human teeth with Nd:YAG laser beam in the picosecond time domain (Serafetinides *et al.*, 1999) has not been sufficiently described in the literature in comparison to the nanosecond domain (Frankline *et al.*, 2005). In this paper, our emphasis is on the study of the effects of a picosecond laser emitting in the visible region (532 nm) on human teeth. Special attention was paid to morphological surface modifications of human teeth at given laser energy fluence.

MATERIALS AND METHODS

Tooth Sample

A total of 10 extracted human teeth belonging to 14–20 years old patients from Sweden were used during the experiment, non-caries premolars were transversally sectioned by a slow speed diamond disk (Model 150, MTI Corporation, Richmond, CA), which are parallel to the occlusal surface. Water is used as a coolant during the slicing of the tooth to prevent damage, due to friction. The image of the sample, prior to laser irradiation, is shown in Figure 1. The thickness of each sample was about 1 mm. The preparation process resulted in a relatively rough surface.

Teeth were stored in distilled water until the time of the experiment, so that the structure of the tooth was not disturbed (Strawn *et al.*, 1996). Slices of the teeth were also stored in water until the start of the experiment.

The Laser System

Human teeth were irradiated by focusing the laser beam using a glass lens of 10 cm focal length. The angle of incidence of the beam with respect to the sample surface was near 0°. The irradiation was carried out in air, at atmospheric pressure of 1013 mbar, and standard relative humidity.

The laser employed is an active passive mode-locked Nd:YAG system (Model SYL P2, Quanta System Srl. Solbiate, Italy), which was characterized by Faeov *et al.* (2004), and used for ablation studies (Gakovic *et al.*, 2007; Trtica *et al.*, 2007*a*, 2007*b*). It includes an oscillator, an amplifier, and a non-linear crystal (KD*P) to convert laser emission to second harmonic (532 nm). Pulse duration of about 40 ps is obtained by using a saturable absorber dye and an acousto-optic modulator. The laser was operated with a typical repetition rate of 1 Hz at 532 nm wavelength. Thanks to the use of an intra-cavity pin-hole, the emitted mode was quasi-TEM_{00}.

Diagnostics Techniques

Various analytical techniques were used for the characterization of the human teeth before and after laser irradiation. The surface characteristics were monitored by optical (OM) and by scanning electron microscope (SEM). Teeth, as non-conductive samples, must be prepared before the SEM analysis. In our case, first the samples were dehydrated in graded solutions of ethanol and later a 20 nm gold coating was deposited onto the surface by using conventional sputter coater. This conductive layer was needed to minimize charging and beam drift during imaging scanning. The SEM was typically operated at 20 kV and the beam current was varying in the interval of 15–40 nA under a pressure of 10^{-6}–10^{-8} mbar.

The SEM was also coupled to an energy dispersive analyzer (EDAX) for determining the surface compositions of the

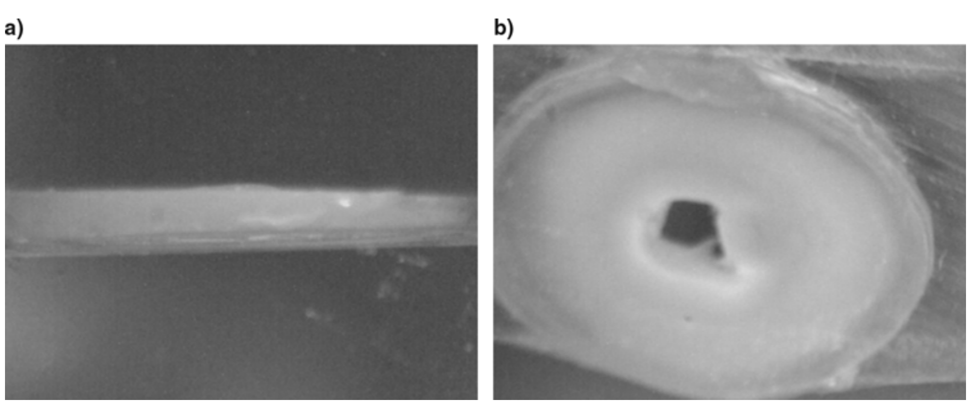

Fig. 1. Transverse section of the prepared tooth sample. The thickness of each sample was about 1 mm.

https://doi.org/10.1017/S0263034609000159 Published online by Cambridge University Press

sample. Optical confocal microscopy (OCM) was employed in the characterization process in the reflection mode, primarily for specifying the geometry of the ablated area and measuring the depth of the crater after coating with gold. In addition, the diameter of each crater depth was measured using the OCM. In this paper, we concentrate on SEM results only.

RESULTS AND DISCUSSION

Morphological changes induced by the action of lasers on human teeth targets were studied *versus* laser beam characteristics: energy fluence and number of accumulated successive pulses.

Morphological changes of the human teeth for one and three accumulated laser pulses at 532 nm are presented in Figures 2 to 4, respectively. The laser energy fluence (Φ) during the experiment was kept constant at $\cong 11\ \mathrm{J/cm^2}$; such fluence induced significant surface modifications on human teeth. The results of the induced modifications can be presented as follow.

Interaction of picosecond laser pulses at the given fluence creates damage on enamel as well as dentine surfaces (Fig. 2). Normally, the accumulation of numerous pulses resulted in an enhancement of the modification (primarily diameter and depth of the ablation area were increased). When the laser was focused on the tooth surface, bright plasma was clearly visible, pointing toward the laser source, and a typical sparking noise was heard. In this context, the finding of Serafetinides *et al.* (1999) is in good agreement with results that show morphology changes in the fundamental and the second harmonic Nd:YAG laser wavelengths, but the most prominent modification was recorded for 532 nm (Serafetinides *et al.*, 1999).

Changes in Enamel

Detailed morphology changes on enamel are shown in Figures 3 and 4. On enamel (Fig. 3B), surface features can be characterized as: (1) appearance of a crater in the central zone of interaction and (2) existence of a diffuse periphery characterized by a cauliflower-like morphology. The crater has a conical form with a depth of 4 μm for one pulse, and 17 μm depth for three successive accumulated pulses; the crater diameter is more or less 300 μm.

Changes in Dentine-Enamel Junction

The effect of laser irradiation on the dentine-enamel junction is shown in Figures 3C1–3C4 and Figure 4B. SEM analysis showed that on the enamel and dentine side, different morphology structures were produced. Features on the enamel

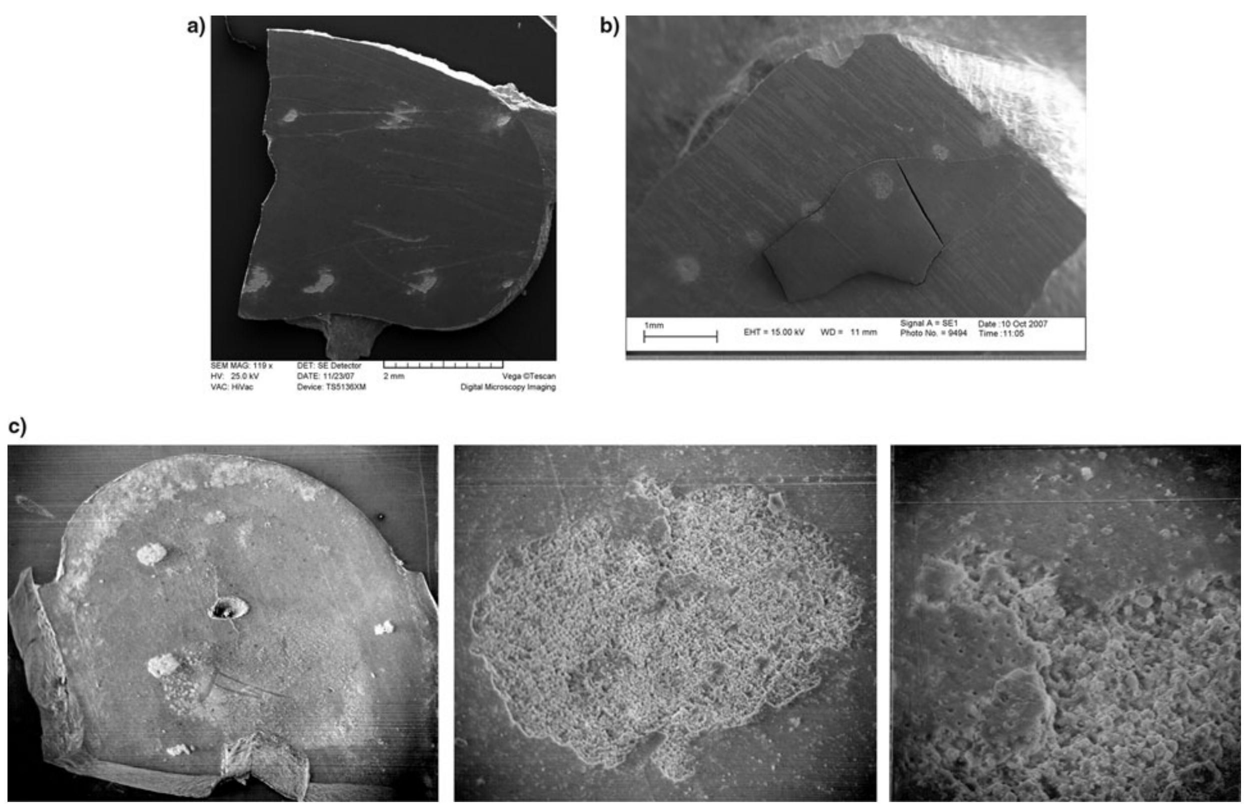

Fig. 2. View of human teeth after irradiation with picosecond Nd:YAG laser at 532 nm with fluence $F = 11\ \mathrm{J/cm^2}$; SEM analysis. (**a**, **b**) View of enamel-dentine after irradiation with one and three pulses, respectively. (**c**) Only dentine after one pulse (in each position). Interaction of picosecond laser pulses at the given fluence creates the damage at enamel as well as at the dentine surface.

https://doi.org/10.1017/S0263034609000159 Published online by Cambridge University Press

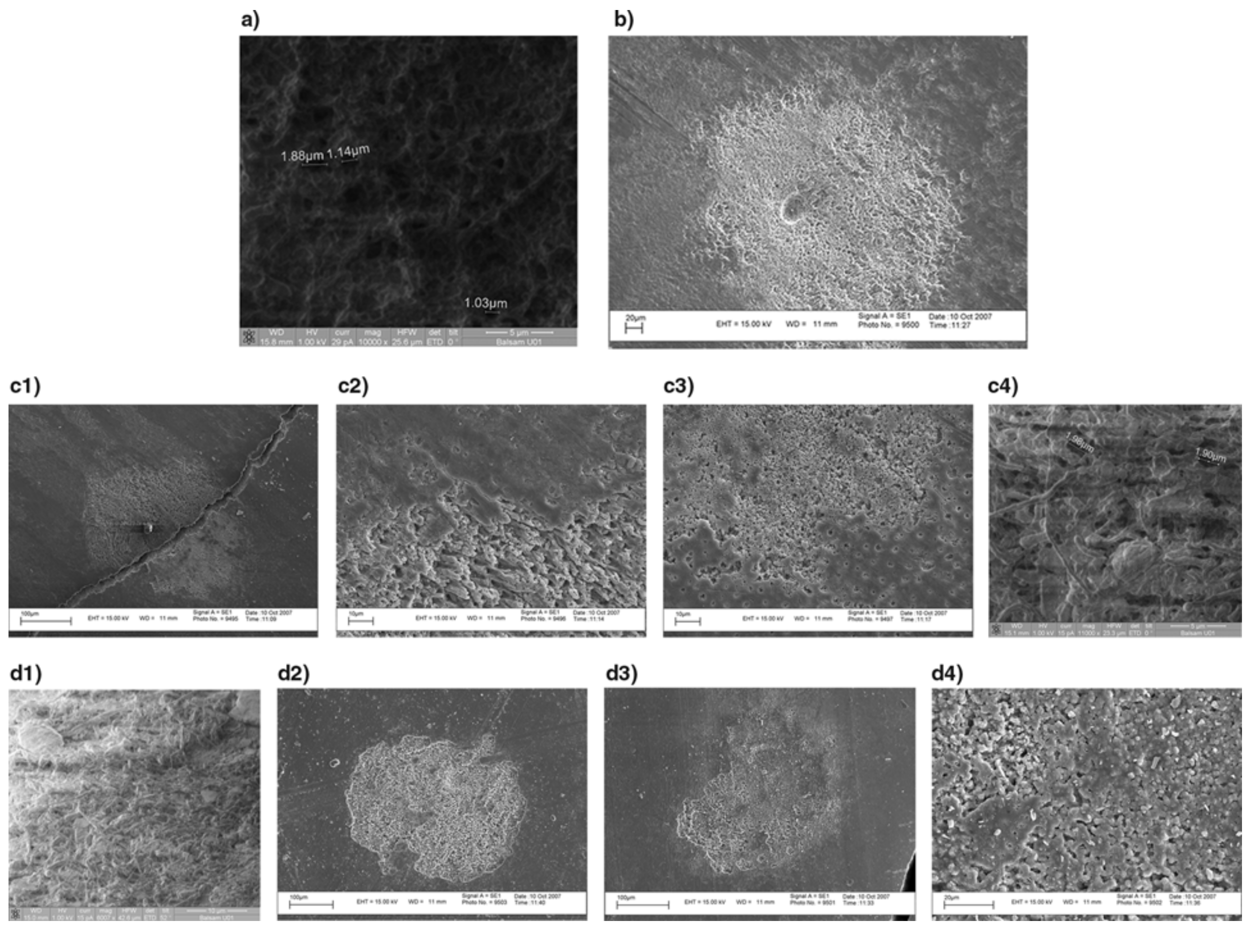

Fig. 3. Picosecond Nd:YAG laser induced changes on human tooth. SEM analysis; $F = 11\ \mathrm{J/cm^2}$; 532 nm. (**a**) view of enamel before laser irradiation, (D1) view of dentine before laser irradiation, (**b**) enamel after three pulses, (**c**) enamel-dentine junction after three pulses, (C1) enamel-dentine border, (C2, C3, and C4) view of enamel, dentine, and channel, (D2) dentine after irradiation with one pulse, (D3) dentine after irradiation with three pulses, (D4), same as D3 but with larger magnification.

side posses a conical-like character (Fig. 2C3). Besides some holes exist. On the dentine side (Fig. 3C3), these features are lower in dimensions (micron and sub-micron range) with typical scales of SEM, and usually there are no holes in the damage area. Also on the dentine surface, sporadic islands of melted and resolidified materials can be detected (Fig. 3C3). The periphery is relatively sharp whereas, at larger distance from the edge of the irradiated area, some pores can be clearly recognized. These represent the dentinal tubules on the non-irradiated surface. The ablation depth on enamel and dentine in the area of the junction was different and typically amounted to 13 μm and 32 μm, respectively, after accumulation of the three pulses per position.

The difference in the recorded morphology, after laser irradiation, on the dentine-enamel junction can be primarily attributed to the different composition. Enamel includes about 96% hydroxyapatite ($Ca_{10}(PO_4)_6(OH)_2AH$), 4% protein (organic material) as well as water, which makes it mechanically hard and highly resistant to wear. Dentine is the supporting structure that lies underneath enamel, primarily composed of hydroxyapatite (70%), water and organic material like proteins (30%). Less mineralized tissues provide the tooth with toughness required to resist fracture when it is subjected to masticatory stresses. The morphology of the junction between enamel and dentine, after laser irradiation, is presented in Figures 3C4 and 4B. The non-irradiated junction (Fig. 4A) is filled up with collagen fibers and the junction channel can not be seen. Examination of the interface between enamel and dentine reveals closely arranged scalloped-shaped outlines. Several collagen fibrils that are projected longitudinally from the dentine matrix seem to converge to form a coarse collagen bundle of 80–120 nm in diameter, these are the Kroff fibers.

Irradiation with a picosecond laser causes the removal of collagen fibers from the channel as well as its modification. Since the images in Figures 3C4 and 4B correspond to three accumulated shots, we can suppose that the first pulse removes the collagen fibers, whereas the other pulses induce the modification of the channel. The bottom of the channel shows transversely oriented needles whereas the surface shows some cracking-like effect.

https://doi.org/10.1017/S0263034609000159 Published online by Cambridge University Press

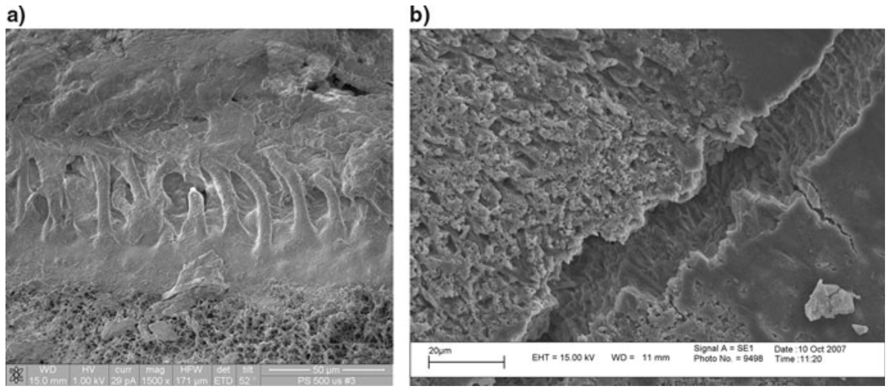

Fig. 4. View of enamel-dentine junction before (**a**) and after laser irradiation with three pulses per position (**b**). SEM analysis; $F = 11$ J/cm^2, $\lambda = 532$ nm. The non-irradiated junction (Fig. 4A) is filled up with collagen fibers and the junction channel can not be seen.

Changes in Dentine

Surface modifications of dentine, away from the enamel-dentine junction, are shown in Figures 3D2–3D4. Even one laser pulse was enough to induce significant ablation (Fig. 3D2) of the dentine. The region of the actual crater ablation extends to about 400 μm in diameter, and the diameter of the visible surface modification in dentine is 450 μm (i.e., it overlaps the diameter of the laser beam). The depth of ablation was 17 μm for one pulse per position. Generally, changes on dentine can be summarized as: (1) efficient ablation, (2) sharp periphery, (3) presence of melted and resolidified regions in the central damage zone, and (4) the tissue modification at the bottom of the crater shows no crack on the floor, with the presence of spherical shape particles of a few micrometers in diameter, which are formed due to hydrodynamic sputtering.

In general, the covered and exposed dentinal tubules, which are present within the area of the study, show no sign of damage after laser irradiation.

CONCLUSIONS

The interaction of 532 nm Nd:YAG laser radiation, at fluence of about 11 J/cm^2, with human teeth is very efficient. Various surface morphologies on enamel and dentine were recorded. Features on enamel (away from the dentine-enamel junction) include a crater in central part (conical form) and cauliflower morphology at periphery. Instead at dentine (away from the dentine-enamel junction), the crater shows a different shape, and a relatively sharp periphery. Analyses of the dentine-enamel junction area and of regions far from the junction showed that the morphology of enamel alone or dentine alone (i.e., in locations more distant from the dentine-enamel junction area) was different. The enamel and dentine junction areas showed features like conical shape craters with sporadic melted resolidified islands. Finally, the junction channel, after irradiation, showed a removal of collagen fibers, and a needle-like bottom structure.

Generally, this investigation showed that picosecond Nd:YAG laser radiation can induce ablation on teeth surfaces almost instantaneously, meaning that by adjusting the focal spot of the laser beam, a precise cutting of the tooth can be achieved. Roughness of the inner surface and the wall of the craters, and bleached borders are beneficial to provide enough retention for the restorative (filling) material.

The appearance of plasma, in front of the teeth, indicates relatively high temperatures created above the surface. This may offer sterilizing effects, facilitating contaminant-free conditions during dental treatment.

ACKNOWLEDGMENTS

We would like to express our deep thanks to the Landau network, Centro Volta (LNCV) in particular to Prof. Riccardo Redaelli and Dr. Andrea Plebani for offering the opportunity to accomplish the research work at the University of Milano Bicooca. We acknowledged the kind advice and rich discussion with Milan Trtica (Vinca Institute of Nuclear Sciences, Belgrad, Serbia). In the same regards, we would like to thank the staff at the Istituto di Istologia, Embriologia and Neurocitologia for preparing and cooperation during scanning SEM images. Sincere thanks go to Dr. Noberto Chiodini for his help in preparing the teeth slices.

REFERENCES

Alti, K. & Khare, A. (2006). Low-energy low-divergence pulsed indium atomic beam by laser ablation. *Laser Part. Beam* **24**, 47–53.

Bashir, S., Rafique, M.S. & Ul-Haq, F. (2007). Laser ablation of ion irradiated CR-39. *Laser Part Beams* **25**, 181–191.

Batani, D., Dezulian, R., Redaelli, R., Benocci, R., Stabile, H., Canova, F., Desai, T., Lucchini, G., Krousky, E., Masek, K., Pfeifer, M., Skala, J., Dudzak, R., Rus, B., Ullschmied, J., Malka, V., Faure, J., Koenig, M., Limpouch, J., Nazarov, W., Pepler, D., Nagai, K., Norimatsu, T. & Nishimura, H. (2007). Recent experiments on the hydrodynamics of laser-produced plasmas conducted at the PALS laboratory. *Laser Part Beams* **25**, 127–141.

Batani, D., Stabile, H., Ravsio, A., Lucchini, G., Desai, T., Ullschmied, J., Krousky, E., Juha, L., Skala, J., Kralikova, B., Pfeifer, M., Kadlec, C., Mocek, T., Präg, A., Nishimura, H. & Ochi, Y. (2003). Ablation pressure scaling at short laser wavelength. *Phys. Rev. E* **68**, 067403.

Beilis, I. (2007). Laser plasma generation and plasma interaction with ablative target. *Laser Part. Beams* **25**, 53–63.

Bhaskar, S.N. (1991). *Orbans Oral Histology and Embryology*. St. Louis: C.V. Mosby.

Bussoli, M., Batani, D., Desai, T., Milani, M., Milan, T., Gakovic, B. & Krousky, E. (2007). Study of laser induced ablation with FIB devices. *Laser Part. Beams* **25**, 121–125.

Carlson, S.J. & Krause, D.W. (1985). *Enamel Ultrastructure of Multituberculate Mammals: An Investigation of Variability Contributions from the Museum of Paleeok*. East Lansing: University of Michigan.

Desai, T., Batni, D., Rossetti, S. & Lucchini, G. (2005). Laser induced ablation and crater formation at high laser flux. *Rad. Effects Defects Solids* **160**, 595–600.

Desai, T., Dezulian, R. & Batani, D. (2007). Radiation effects on shock propagation in Al target relevant to equation of state measurements. *Laser Part. Beams* **25**, 23–30.

Desai, T., Batani, D., Bussoli, M., Villa, A.M., Dezulian, R. & Krousky, E. (2008) . Laboratory craters: Modeling experiments for meteorite impact craters? *IEEE Trans. Plasma Sci*. **36**, 1132–1133.

Di Bernardo, A., Batani, D., Desai, T., Courtois, C., Cros, B. & Matthieussent, G. (2003). High intensity ultra short laser induced ablation of metal targets in the presence of ambient gas. *Laser Part. Beams* **21**, 59–64.

Faeov, A., Pikuz, T., Magunov, A., Batani, D., Lucchini, G., Canova, F. & Piselli, M. (2004). Bright point X-ray source based on a commercial portable 40 ps Nd:YAG laser system. *Laser Part. Beams* **22**, 373–379.

Fernández, J.C., Hegelich, B.M., Cobble, J.A., Flippo, K.A., Letzring, S.A., Johnson, R.P., Gautier, D.C., Shimada, T., Kyrala, G.A., Wang, Y., Wetteland, C.J. & Schreiber, J. (2005). Laser-ablation treatment of short-pulse laser targets: Towards an experimental program on energetic interactions with dense plasmas. *Laser Part. Beams* **23**, 267–273.

Frankline, S.R., Chauhan, P., Mitra, A. & Thareja, R.K. (2005). Laser ablation of human tooth. *J. Appl. opt*. **97**, 094919.

Gakovic, B., Trtica, M., Batani, D., Desai, T., Panjan, P. & Vasiljevic-Radoyic, D. (2007). Surface modification of titanium nitride film by a picosecond Nd:YAG laser. *J. Opt. A* **9**, 79–80.

Kasperczuk, A., Pisarczyk, T., Kalal, M., Martinkova, M., Ullschmied, J., Krousky, E., Masek, K., Pfeifer, M., Rohlena, K., Skala, J. & Pisarczyk, P. (2008). PALS laser energy transfer into solid targets and its dependence on the lens focal point position with respect to the target surface. *Laser Part. Beams* **26**, 189–196.

Makropoulou, M.I., Serafetinides, A.A. & Khabbaz, M.G. (1996). Dentin ablation measurements in endodontics with HF and CO_2 laser radiation. *SPIE* **2623**, 200–210.

Neev, J., Stabholz, A., Liaw, L., Torabinejad, M., Fujishige, J.T., Ho, P.H., Berns, M.W. (1993). Scanning electron microscopy and thermal characteristics of dentin ablated by a short pulse XeCl laser. *Laser Surg. Med*. **13**, 353–361.

Neev, J., Raney, D.V., Fujishige, J.T., Ho, P.T. & Berns, M.W. (1991). Selectivity and efficiency in the ablation of hard dental tissue with ArF pulsed excimer lasers. *Laser Surg. Med*. **11**, 499–510.

Neev, J., Da Silva, L.B., Feet, M.D., Perry, M.D., Rubenchik, A.M., Stuart, B.C. (1996). Ultrashort pulse lasers for hard tissue ablation. *IEEE J. Quan. Electron*. **2**, 790–800.

Rode, A.V., Gamaly, E.G., Luther-Davies, B., Taylor, B.T., Graessel, M., Dawes, J.M., Chan, A., Lowe, R.M. & Hannaford, P. (2003). Precision ablation of dental enamel using a subpicosecond pulsed laser. *Australian Dental J*. **32**, 233–239.

Schade, W., Bohling, C., Hohmann, K. & Scheel, D. (2006). Laser-induced plasma spectroscopy for mine detection and verification. *Laser Part. Beams* **24**, 241–247.

Schreiber, J. (2005). Laser-ablation treatment of short-pulse laser targets: Toward an experimental program on energetic-ion interactions with dense plasmas. *Laser Part. Beams* **23**, 267–273.

Serafetindes, A.A., Khabbaz, M.G., Makropouloub, M.I. & Kar, A.K. (1999). Picosecond laser ablation of dentine in endodontics. *Laser Med. Sci*. **14**, 168–174.

Stawn, S.E., White, J.M., Marshll, G.W., Gee, L., Goodis, H.E. & Marshall, S.J. (1996). Spectroscopic changes in human dentine exposed to various storage solutions—short term. *J Dent*. **24**, 417–423.

Takuma, S., Tohda, H.,Watanabe, K., Ogiwara, H. & Yanagisawa, T. (1982). Scanning electrum microscopy on ion etching of enamel and dentin. *J. Electron Microscope* **31**, 144–150.

Thareja, R.K. & Sharma, A.K. (2006). Reactive pulsed laser ablation: Plasma studies. *Laser Part. Beams* **24**, 311–320.

Trtica, M., Gakovic, B., Batani, D., Desai, T., Panjan, P. & Radak, B. (2006*a*). Surface modifications of a titanium implant by a picosecond Nd:YAG laser operating at 1064 and 532 nm. *Appl. Surf. Sci*. **253**, 2551–2556.

Trtica, M., Gakovic, B., Maravic, D., Batani, D., Desai, T. & Redaelli, R. (2006*b*). Surface modification of titanium by high intensity ultra-short Nd:YAG Laser. *Mater. Sci. Forum* **518**, 167–172.

Trtica, M., Gakovic, B., Maravic, D., Batani, D., Desai, T. & Redaelli, R. (2007*a*). Surface modifications of crystalline silicon created by high intensity 1064 nm picosecond Nd:YAG laser pulses. *Appl. Surf. Sci*. **253**, 9315–9318.

Trtica, M., Gakovic, B., Radak, B., Batani, D., Desai, T. & Bussoli, M. (2007*b*). Periodic surface structures on crystalline silicon created by 532 nm picosecond Nd:YAG laser pulses. *Appl. Surf. Sci*. **254**, 51377–51381.

Trusso, S., Barletta, E., Barreca, F., Fazio, E. & Neri, F. (2005). Time resolved imaging studies of the plasma produced by laser ablation of silicon in O-2/Ar atmosphere. *Laser Part. Beams* **23**, 149–153.

Veiko, V.P., Shakhno, Ea., Smirnov, V.N., Miaskoski, Am. & Nikishin, G.D. (2006). Laser-induced film deposition by LIFT: Physical mechanisms and applications. *Laser Part. Beams* **24**, 203–209.

Wieger, V., Strassl, M. & Wintner, E. (2006). Pico- and microsecond laser ablation of dental restorative materials. *Laser Part. Beams* **24**, 41–45.

Zip, J.R. & Ten Bosch, J.J. (1993). Theoretical model for the scattering of light by dentin and comparison with measurements. *Appl. opt*. **32**, 411–415.